



Biofilm detachment
by Rune Bakke

A thesis submitted in partial fulfillment of the requirements for the degree of Doctor of Philosophy in Civil Engineering
Montana State University
© Copyright by Rune Bakke (1986)

Abstract:

Monoculture *Pseudomonas aeruginosa* biofilms were modeled by mass balances. Measurable expressions for substrate removal, cellular reproduction, product formation (extracellular polymeric substances), and detachment were extracted from the model to determine kinetics and stoichiometry for the individual processes. This thesis presents a detailed investigation of detachment, the transport of particulate mass across the biofilm/liquid interface.

Methods were developed to monitor biofilm optical thickness and density in situ at various locations in the reactor. The optical thickness was converted into actual (mechanical) biofilm thickness by a geometric analysis of the light path through the sample. Time progressions of biofilm thickness and its spatial variation within the reactor were obtained by this method. Optical film thickness data from the literature were also translated into actual biofilm thickness and compared to the data obtained here. Biofilm optical density was correlated with biofilm cell mass, yielding information regarding biofilm cell mass distribution, time progression, and density. Transmission and scanning electron microscopy were used to relate biofilm morphology to biofilm processes. Liquid phase cell, product, and substrate data, obtained with methods previously published, were analyzed with mass balance equations for the system together with the biofilm data obtained by the new methods. The fundamental processes of accumulation, transport, and transformation were separated and factors of significance to detachment were identified.

P. aeruginosa biofilm thickness reached approximately 35 μm within 24 hours of reactor start-up and remained more or less constant throughout the experiments even though changes in fluid dynamic conditions were imposed on the system during this period. Changes in biofilm composition, interface morphology, and activity were observed throughout the experiments. It was concluded that constant biofilm thickness can serve as the most appropriate boundary condition linking the liquid phase and the biofilm mass balances required to model the detachment process. Alternative boundary conditions, such as constant biofilm density and specific detachment rate proportional to fluid shear force, were not supported by the data.

BIOFILM DETACHMENT

by

Rune Bakke

A thesis submitted in partial fulfillment
of the requirements for the degree

of

Doctor of Philosophy

in

Civil Engineering

MONTANA STATE UNIVERSITY
Bozeman, Montana

June 1986

MAIN LIB.
D378
B179
Cop.2

© COPYRIGHT

by

Rune Bakke

1986

All Rights Reserved

APPROVAL

of a thesis submitted by

Rune Bakke

This thesis has been read by each member of the thesis committee and found to be satisfactory regarding content, English usage, format, citations, bibliographic style, and consistency, and is ready for submission to the College of Graduate Studies.

19 June 1986
Date

W. V. Charvath
Chairperson, Graduate Committee

Approved for Major Department

19 June 1986
Date

Theodore E. Ranz
Head, Major Department

Approved for College of Graduate Studies

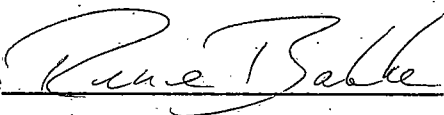
24 June 1986
Date

Henry P. Parsons
Graduate Dean

STATEMENT OF PERMISSION TO USE

In presenting this thesis in partial fulfillment of the requirements for a doctoral degree at Montana State University, I agree that the Library shall make it available to borrowers under rules of the Library. I further agree that copying of this thesis is allowable only for scholarly purposes, consistent with "fair use" as prescribed in the U.S. Copyright Law. Requests for extensive copying or reproduction of this thesis should be referred to University Microfilms International, 300 North Zeeb Road, Ann Arbor, Michigan 48106, to whom I have granted "the exclusive right to reproduce and distribute copies of the dissertation in and from microfilm and the right to reproduce and distribute by abstract in any format."

Signature



Date

19 June 1986

ACKNOWLEDGMENTS

I wish to express my appreciation to the following:

Bill Characklis for providing advice, support, and the research environment where I could reach my goals.

Keith Cooksey, Al Cunningham, Gordon McFeters, and Dan Goodman for their large contributions to my thesis program.

Shari McCaughey, Zbigniew Lewandowski, Robert Kultgen, and Warren Jones for help with my thesis.

Andy, Maarten, Pam, Wendy, Whon Chee, Mukesh, and Ewout for their cooperation.

Gordon Williamson and Stuart Aasgaard for technical assistance.

The staff and students of the Civil Engineering, Chemical Engineering, and Microbiology Departments whom have contributed to my education.

All my friends whom have made my student life so enjoyable.

Montana State University Engineering Experiment Station, National Science Foundation, Office of Naval Research, and Statens Laanekasse for financial support.

TABLE OF CONTENTS

	Page
LIST OF TABLES	vii
LIST OF FIGURES.....	viii
ABSTRACT.....	xi
INTRODUCTION.....	1
Goal and Objectives.....	4
LITERATURE REVIEW.....	5
Detachment.....	5
Biofilm Models.....	6
Erosion.....	9
Fluid Shear Stress.....	9
Biofilm Mass.....	10
Sloughing.....	10
Reactor Performance.....	12
Biofilm Properties.....	14
Biofilm Composition.....	14
Organism.....	17
Biofilm-Liquid Interface.....	17
THEORY.....	20
Model.....	20
Mass Balance.....	20
Phase Separation.....	21
Sensitivity Analysis.....	23
Process Rates.....	27
Biofilm Composition.....	30
EXPERIMENTAL METHODS.....	35
Experimental Apparatus.....	35
Operating Conditions.....	36
Experimental Procedures.....	46
Analytical Methods.....	49
Biofilm Thickness.....	49
Optical Density.....	53
Statistical Methods.....	53

TABLE OF CONTENTS (Continued)

	<u>Page</u>
RESULTS.....	54
Data Correlation.....	54
Biofilm Refractive Index.....	54
Light Scattering vs. Biomass.....	55
Progression of Biofilm Variables.....	56
Biofilm Thickness.....	56
Light Scattering by Biofilms.....	62
Fluid Shear Stress.....	63
Progression of Liquid Phase Variables.....	63
Substrate Concentration.....	63
Cell Concentration	66
Extracellular Polymeric Substances (EPS).....	66
DISCUSSION.....	69
Biofilm Detachment.....	69
Specific Cellular Detachment Rate.....	69
Biofilm Thickness.....	70
Biofilm Roughness.....	78
Biofilm Composition.....	85
Transitions.....	87
Biofilm Aging.....	89
Specific Cellular Growth Rate.....	91
Biofilm Accumulation.....	94
Specific Accumulation Rate.....	94
Steady State.....	96
Modeling.....	100
CONCLUSIONS.....	103
NOMENCLATURE.....	106
BIBLIOGRAPHY.....	108
APPENDIX.....	114

LIST OF TABLES

<u>Table</u>		<u>Page</u>
1	Relevant kinetic and stoichiometric coefficients for <u>P. aeruginosa</u> .	18
2	Mass balances for biofilm reactor with general terms for process rates.	25
3	Mass balances for biofilm reactor including kinetic expressions for specific rates (Bakke et al., 1984).	26
4	Dimensions of the MRTR.	40
5	Reactor components and dimensions.	41
6	Fraction of substrate removed (reported as mean \pm standard deviation of four samples) at various recycle rates in liquid phase mass transfer study of MRTR.	45
7	Composition of Nutrient Solution.	47
8	Analytical methods applied.	50
9-25	Raw data.	114

LIST OF FIGURES

<u>Figure</u>		<u>Page</u>
1	Schematic representation of two phase biofilm system described by Equations 10-15. Bulk transport, substrate diffusion, cell and EPS production, and detachment are processes included. The coordinate system defined for this study is illustrated.	24
2	Specific cellular growth rate, m , modeled as a saturation function of substrate concentration and product formation rate modeled as the sum of a growth and a non-growth associated term, plotted vs. substrate concentration.	34
3	Schematic diagram of experimental system including flow and temperature control for gas and liquids.	37
4	Mixed rectangular tube reactor (MRTR). Biofilm measurements and samples were obtained at locations labeled 1-8.	38
5	Cross section view of rectangular tube. A-B-C-D are light paths for biofilm thickness and optical density measurements. Scale indicated along the y-axis. Biofilm thickness profile measurements were taken along the y-axis at marked positions .250 mm apart.	39
6	Fluid shear stress progression in Experiment I. Continuous flow operation started at time zero.	42
7	Fluid shear stress progression in Experiment II. Continuous flow operation started at time zero.	43
8	Fluid shear stress progression in Experiment III. Continuous flow operation started at time zero.	44
9	Calibration curve for biofilm cell carbon areal density vs. light scattering by the biofilm measured as absorbance at wave length = 450 nm. Line represents best linear fit ($R^2=0.88$).	57

LIST OF FIGURES (Continued)

<u>Figure</u>		<u>Page</u>
10	Calibration curve for liquid phase cell carbon concentration vs. light scattering in the liquid phase measured as absorbance at wave length ₂ = 450 nm. Line represents best linear fit ($R^2=0.94$).	58
11	Biofilm thickness progression in Experiment I.	59
12	Biofilm thickness progression in Experiment II.	60
13	Biofilm thickness progression in Experiment III.	61
14	Progression of biofilm optical density, measured as absorbance at locations 1-8 (Figure 4), in Experiment III.	64
15	Progression of liquid phase substrate concentration, C_S (x - influent, □ - effluent) in Experiment III. Data points represents the average of two samples.	65
16	Liquid phase cell mass, C_{M1} , calculated from light scattering data (effluent optical density) in Experiment II.	67
17	Liquid phase cell (□) and EPS (x) fraction of particulate organic carbon (POC) in the effluent in Experiment III.	68
18	Progression of specific cellular detachment rate, determined according to Equation 17 from optical density data.	71
19	Scanning electron micrograph (SEM) of biofilm at the completion of Experiment III.	73
20	Scanning electron micrograph (SEM) of biofilm at the completion of Experiment III.	74
21	Scanning electron micrograph (SEM) of biofilm at the completion of Experiment III.	75
22	Transmission electron micrograph (TEM) of biofilm at the completion of Experiment III.	76

LIST OF FIGURES (Continued)

<u>Figure</u>		<u>Page</u>
23	Transmission electron micrograph (TEM) of biofilm at the completion of Experiment III.	77
24	Optical photo micrograph of biofilm-liquid interface at 50 hours. Corresponding to Figure 25.	79
25	Biofilm thickness profile along the y-axis (i.e. perpendicular to bulk liquid flow direction) at 50 hours. Corresponding to Figure 24.	80
26	Optical photo micrograph of biofilm-liquid interface at 272 hours. Corresponding to Figure 27.	82
27	Biofilm thickness profile along the y-axis (i.e. perpendicular to bulk liquid flow direction) at 272 hours. Corresponding to Figure 26.	83
28	Progression of standard deviation of nine biofilm thickness samples in Experiments II and III.	84
29	Measured cell and EPS fractions of biofilm carbon (POC) in a) this study, and b) Trulear's (1983) experiments.	86
30	Progression of liquid phase specific cellular growth rate, m_1 , calculated from Equation 20 and substrate data (Figure 15).	93
31	Specific biofilm cell accumulation rate progression in Experiments II and III, calculated as the l.h.s. of Equation 16 from biofilm optical density data.	95
32	Specific biofilm cell accumulation rate progression in Experiments II and III on a natural logarithmic scale. Data from Figure 31, excluding data obtained during recycle rate transitions.	97

ABSTRACT

Monoculture Pseudomonas aeruginosa biofilms were modeled by mass balances. Measurable expressions for substrate removal, cellular reproduction, product formation (extracellular polymeric substances), and detachment were extracted from the model to determine kinetics and stoichiometry for the individual processes. This thesis presents a detailed investigation of detachment, the transport of particulate mass across the biofilm/liquid interface.

Methods were developed to monitor biofilm optical thickness and density in situ at various locations in the reactor. The optical thickness was converted into actual (mechanical) biofilm thickness by a geometric analysis of the light path through the sample. Time progressions of biofilm thickness and its spatial variation within the reactor were obtained by this method. Optical film thickness data from the literature were also translated into actual biofilm thickness and compared to the data obtained here. Biofilm optical density was correlated with biofilm cell mass, yielding information regarding biofilm cell mass distribution, time progression, and density. Transmission and scanning electron microscopy were used to relate biofilm morphology to biofilm processes. Liquid phase cell, product, and substrate data, obtained with methods previously published, were analyzed with mass balance equations for the system together with the biofilm data obtained by the new methods. The fundamental processes of accumulation, transport, and transformation were separated and factors of significance to detachment were identified.

P. aeruginosa biofilm thickness reached approximately 35 μm within 24 hours of reactor start-up and remained more or less constant throughout the experiments even though changes in fluid dynamic conditions were imposed on the system during this period. Changes in biofilm composition, interface morphology, and activity were observed throughout the experiments. It was concluded that constant biofilm thickness can serve as the most appropriate boundary condition linking the liquid phase and the biofilm mass balances required to model the detachment process. Alternative boundary conditions, such as constant biofilm density and specific detachment rate proportional to fluid shear force, were not supported by the data.

INTRODUCTION

Biofilms are microbial populations and their matrices of noncellular material accumulated on surfaces submerged in a liquid phase. The biofilms in this study consisted of bacterial cells and extracellular polymeric substances (EPS). The part of the biofilm exposed to the liquid phase, termed the surface film, is of primary significance to biofilm modeling since all mass transfer between biofilm and liquid phase occurs here. These transfer processes are the main distinction between biofilm systems and dispersed microbial systems. The base film is the continuous biofilm matrix between the surface film and the substratum.

Detachment is defined as the transfer of particulate mass (e.g. cells and EPS) from the biofilm to the bulk liquid phase. Detachment due to shear forces results in continuous removal of individual cells and small particles at the biofilm liquid interphase and is referred to as erosion. Sporadic detachment of larger portions of biofilm due to physiochemical conditions within the biofilm is termed sloughing. Erosion and sloughing are treated as separate processes because evidence suggests that the causes of erosion and sloughing can be distinguished. The distinction

is somewhat arbitrary and most systems probably experience both kinds of detachment. Erosion and sloughing are also treated differently because they may have significantly different effects on biofilms.

Understanding of biofilm detachment has relevance to biofilm reactor operation, biofouling treatment, and understanding of biofilm processes in general. Biofilm detachment can be the rate limiting process which determines the metabolic state (average specific cellular growth rate) of steady state biofilms (Bakke et al., 1984). Understanding of biofilm detachment is, therefore, not only necessary to predict biofilm behavior, but this knowledge may also serve as a tool to control biofilm activity. The central role of detachment processes in composition and performance of multi-species biofilm reactors, and the need for further investigation of detachment processes have been demonstrated through theoretical analysis of biofilm reactors (Howell and Atkinson, 1976; Wanner and Gujer, 1985).

The importance of understanding biofilm processes in general is emphasized by the increasing number of applications of biofilm reactors for biological transformation processes. Biofilm modeling can aid design and operation of such bio-reactors.

Biofilms can also lead to costly problems, such as excessive heat transfer resistance and fluid frictional losses in process equipment. Improved methods for biofilm

monitoring, analysis, and modeling can aid in development of treatment programs to maintain performance of such equipment.

Very little qualitative and quantitative information regarding detachment is available, in spite of the apparent significance of detachment in biofilm reactors. This study was, therefore, designed to study detachment in monoculture biofilms. Biofilm properties, metabolic conditions, and fluid dynamic conditions in Pseudomonas aeruginosa biofilm reactors were monitored to identify factors of significance to biofilm detachment. Biofilm properties monitored were biofilm thickness, density, structure, and interface appearance. The interface of primary interest is the biofilm-liquid interface, and its appearance was characterized by its surface roughness. Electron and light microscopy were used extensively to investigate biofilm structure, particle distribution, and interface roughness. Substrate consumption and cellular growth rate were monitored as measures of metabolic conditions. Recycle flow rate was controlled and friction imposed on this flow by the biofilm was monitored as pressure drop. Fluid shear stress acting on the biofilm due to liquid phase flow was, thereby, measured. Since most of these measurements were conducted throughout the experiments they serve as an investigation of biofilm aging, and its effect on detachment. No previous monoculture biofilm experiment reported in the literature

lasted longer than two weeks. Long-term biofilm behavior was, therefore, unknown.

Goals and Objectives

The goal of this study was to identify factors of significance to biofilm detachment. Several variables were monitored in pursuit of the goal, yielding information regarding a) biofilm boundary conditions b) biofilm stability (steady state conditions), c) biofilm properties, d) new methods for biofilm characterization, and e) long term biofilm behavior or aging.

LITERATURE REVIEW

Detachment

Detachment is the transfer of particulate mass, such as cells and EPS, from the biofilm to the liquid phase. Bakke et al. (1984) demonstrated that detachment can be the process which controls the cells metabolic state (e.g. specific cellular growth rate) in a biofilm reactor. They also demonstrated that the kinetic and stoichiometric coefficients describing biological transformations in a chemostat apply as well in biofilms. This implies that mass transport processes are the only processes which conceptually distinguish biofilm systems from dispersed bioreactors. Given significant information regarding transport of dissolved materials in biofilms (Atkinson and Davies, 1974), this study focused on particulate transport across the biofilm-liquid interface. Information available in the literature was analyzed to determine which factors may be of primary significance to detachment of particulates (i.e. cells and EPS) and to design experiments to further quantify detachment processes.

Erosion and sloughing were distinguished in the analysis of detachment because they, by definition, have different causes. Erosion is the continuous removal of small particles

from the biofilm at the biofilm-liquid interface due to fluid shear stress. Sloughing is intermittent detachment of large pieces of biofilm due to conditions within the biofilm. The two processes may also have significantly different effects on biofilms. Most biofilms probably experience both erosion and sloughing, but distinguishing the two processes in experiments may be difficult. Erosion at the biofilm surface is a continuous function with only indirect effects on the deeper layers of the film. Sloughing, on the other hand, can directly influence the film at any depth by removal of multiple layers in single events. This may alter the local environment drastically (e.g. expose a previously anaerobic layer to oxygen), and it may change biofilm morphology, causing significant roughness which can alter mass and momentum transfer rates. Separation of erosion and sloughing in this study was accomplished by imposing conditions which favor erosion, making detachment due to sloughing insignificant, as described in detail in the experimental methods section.

Biofilm Models

Biofilms are inherently heterogeneous since gradients are the driving force for transport of dissolved substrate and products from the liquid phase into and out of biofilms (i.e. diffusion gradients). Measurements of temporal and

spatial gradients are difficult at present. To experimentally separate the detachment process from the transformation processes in biofilms, it is, therefore, necessary to reduce the level of inhomogeneity so that the biofilm can be assumed to be homogeneous in the particulate mass balance analysis. Such homogeneity in terms of cell, EPS, and substrate distribution in biofilms was obtained in monoculture biofilms (Trulear, 1983)

Wanner and Gujer (1985) developed a biofilm model which account for gradients in the biofilm by dividing the biofilm into several layers perpendicular to the diffusion gradients. Each layer is treated as individual phases (see Theory chapter) and appropriate boundary conditions account for the interaction between phases. The boundary condition which couples the liquid phase cell mass balance and the cell mass balance for the biofilm layer at the biofilm-liquid interface is net cellular detachment. Wanner and Gujer stated that a large variety of boundary conditions can be applied to model detachment in their numerical simulation of biofilm processes. Selecting the most appropriate expression for detachment must be based on experimental evidence. Trulear and Characklis (1982) found that biofilm erosion may be influenced by fluid shear stress, biofilm density, and biofilm thickness. These observations served as a basis for the present study, which was designed to evaluate the influence of these variables on detachment.

Identifying an appropriate boundary condition for monoculture biofilm detachment modeling based on fluid shear stress, biofilm density, and biofilm thickness data was, therefore, a major objective in this study.

Monoculture biofilms studied by Trulear (1983) and Bakke et al. (1984) were assumed to be homogeneous because they developed insignificant gradients in terms of the mass balance analysis. This simplified the biofilm reactor system significantly, as it consisted of only two homogeneous phases (liquid and biofilm phase), and quantitative measurements of the fundamental processes of significance were obtained. Manipulations of the mass balance equations require to obtain measurable expressions for specific cellular growth, detachment, and accumulation rates are described in detail in the Theory chapter. Kinetic and stoichiometric coefficients obtained in "homogeneous" biofilms have been applied to Wanner and Gujer's (1985) heterogeneous model to simulate monoculture biofilm behavior (Wanner, personal communication). This simulation is described in more detail in the Theory and the Discussion chapters.

Monoculture biofilms in the present study were developed under conditions similar to those applied by Trulear (1983) to minimize the level of biofilm inhomogeneity. Separation of transformation and detachment processes was thereby

possible, and factors of significance to detachment were identified.

Erosion

Fluid Shear Stress. Erosion is defined as the continuous removal of small particles from the biofilm at the biofilm liquid interface due to fluid shear stress from the bulk liquid. The friction imposed by the biofilm on the liquid phase imposes as a shear force on the biofilm. The kinetic energy of the fluid is dissipated through breakage of physical bonds in the biofilm resulting in detachment. Bakke et al. (1986) correlated mixed culture biofilm mass detachment data (Trulear and Characklis, 1982) to fluid shear stress at the biofilm/liquid interface, τ , in a turbulent system by the following equation:

$$r_d = k_d \tau \quad 1$$

where r_d is the specific biofilm detachment rate [t^{-1}] and k_d is a detachment coefficient [$t^{-1} P^{-1}$].

Previous monoculture biofilm experiments were conducted in turbulent flow reactors at constant t (Trulear, 1983; Turakhia, 1986). Trulear's monoculture (*P. aeruginosa*) biofilm experiments were modeled assuming specific detachment rate to be constant (Bakke et al., 1986). To make

the model applicable to systems experiencing fluid dynamic conditions different from those used in previous experiments, it is necessary to determine the effect of fluid dynamics on biofilm erosion. Fluid shear force was, therefore, the control variable in this study, regulated through step functions in fluid recycle rate.

Biofilm Mass. Rittmann (1982) presented equations by which detachment rate can be calculated for various experimental systems and conditions assuming that Equation 1 is valid. He also found that a linear relationship between total biomass detachment rate, $X r_d$, and biofilm mass, X , is a reasonable approximation for the data presented by Trulear and Characklis (1982). Data obtained in monoculture (Pseudomonas aeruginosa) biofilms by Trulear (1983) can also be approximated by a linear relationship between total cellular detachment rate, $C_{M2} r_{dM}$, and biofilm cell mass, C_{M2} (Bakke et al., 1984). Specific cellular detachment rate, r_{dM} , appeared to be independent of biofilm cell concentration, C_{M2} , in Trulear's experiments (Bakke et al., 1986).

Sloughing

Sloughing is defined as intermittent detachment, frequently of large pieces of biofilm, due to conditions within the biofilm. These conditions may evolve slowly and

cause sloughing at random, or they may be triggered by transitions in the environment.

Howell and Atkinson (1976) developed a model for intermittent sloughing triggered by substrate limitation in the biofilm. Experimental data supporting their theory is, however, not available. Even though substrate and nutrient limitations may play a role in sloughing, it is not evident that they actually trigger the detachment. Several other factors, such as polymer gel (EPS) strength and density, may play a significant and varying role in sloughing. Gas bubble formation has, for example, been observed as a major cause of sloughing in denitrifying biofilms (la Cour Jansen, 1983). A quantitative correlation between nitrogen production and sloughing was not reported, probably because other factors influencing internal and external mass transfer were not controlled or monitored. Wanner and Gujer (1985) concluded that direct observation of temporal and spatial gradients in biofilms are required to explain sloughing but these measurements are difficult at present.

Some quantitative information is available regarding sloughing caused by transients. Turakhia et al. (1983) altered the free calcium, Ca^{++} , available for biofilms by calcium chelation, and observed immediate biofilm sloughing of both cells and EPS. Quantitative data relating detachment rates for both cells and EPS to calcium concentration was obtained. The sloughing was presumably caused by removal of

calcium important in the biofilm structure.

Substrate transitions occur frequently in wastewater treatment plants. Such transitions can have negative effects on bioreactor performance, decreasing effluent quality (Storer and Gaudy, 1969; Der Yang and Humphrey, 1975; Bakke, 1983; Rozich and Gaudy, 1985). Bakke (1983) found that the initial response by mixed culture biofilms to step increases in substrate (glucose, lactose, and lactate) loading rates (imposed by doubling influent substrate concentration) was EPS sloughing. Increased biofilm cell detachment was not detected. Therefore, substrate transitions caused selective sloughing of a specific fraction of the biofilm which lasted for a few minutes. The biofilms adapted to increased substrate loading rate conditions by increased metabolism and cell reproduction and re-established steady state within hours.

Reactor Performance

Effects of detachment on reactor performance is reviewed starting with the well-studied homogeneous monoculture biofilms developed by Trulear (Trulear, 1983; Bakke et al., 1984). The average specific cellular reproduction rate, m , in the biofilm was found to be proportional to specific cellular detachment rate. The biofilms investigated were exposed to high fluid shear stress ($\tau = 3.5$ Pa), but caused

no detectable increase in fluid frictional resistance (i.e. a relatively smooth biofilm-liquid interface) (Trulear, 1983), suggesting that erosion was the dominating detachment process. These biofilms were also quite homogeneous [effectiveness factors for diffusion, calculated according to Atkinson and Davies (1974), were greater than 0.9 in all experiments]. So sloughing due to substrate or nutrient limitations was not expected since lack of homogeneity may be a prerequisite for sloughing (Howell and Atkinson, 1976). It was demonstrated in these experiments that steady state specific cellular growth rate, μ , was a direct function of detachment rate but independent of influent substrate concentration.

Regulating detachment may serve as a tool to control and optimize bioreactor processes, since the specific cellular growth rate is so strongly influenced by detachment rate in biofilm reactors (Bakke et al., 1984). Substrate removal is, for example, influenced by detachment rate, since it is closely related to the growth rate of the organisms (Monod, 1942). Product formation is also a function of the cellular growth rate (Luedeking and Piret, 1959; Mian et al., 1978) and can, as suggested for substrate removal, be regulated through detachment control. Given kinetic and stoichiometric coefficients for growth and product formation, and a valid biofilm model, an optimal detachment rate for a given process may be calculated.

In the slightly more complex case where diffusion limitation is significant, average growth rate in the biofilm is still equal to detachment rate at steady state, but its value is less than that calculated from bulk liquid phase substrate concentration (Atkinson and Davies, 1974). It is also no longer possible to analytically determine an optimum detachment condition for a given process due to inhomogeneity (gradients in the film). Given diffusion conditions (biofilm density, thickness, etc.) an optimal operation range may still be determined by accounting for diffusion gradients in the film. This may be accomplished by introducing an effectiveness factor for diffusion limitations, f_D , according to Atkinson and Davies (1974). Alternatively, diffusion gradients in biofilms can be accounted for by dividing the biofilm into several phases (layers perpendicular to the diffusion gradients) within which gradients may be neglected (Wanner and Gujer, 1985).

The effects of detachment on more complex systems such as multi-species and multi-layer biofilms have been analyzed theoretically by Wanner and Gujer (1984). They emphasized the lack of quantitative information necessary to make specific predictions. By comparing extreme cases of sloughing and erosion their model demonstrated that detachment mechanisms play an important role in multi-species biofilm progression, composition, and behavior. Theoretical as well as experimental work on detachment in

multi-species biofilms is required to quantify the effect of detachment on biofilm behavior.

Biofilm Properties

Biofilm Composition

The effect of fluid shear stress on biofilm detachment depends on the physical properties of the biofilm. It is reasonable to assume that a smooth, dense film with a strong structure will experience less erosion than a weak and rough film. The quality and quantity of extracellular polymeric substances (EPS) may strongly influence detachment rates, due to its structural role in microbial aggregates. Quantitative information regarding the role of EPS on detachment rates is unavailable, but significant qualitative information regarding EPS production and biofilm accumulation is available.

A variety of chemical structures is represented in EPS produced by bacteria (Sutherland, 1982). They are usually considered to be carbohydrate with acidic groups (Corpe et al., 1976; Fletcher and Floodgate, 1973), amino groups (Baier, 1975), and sometimes associated with proteins (Corpe et al., 1976). P. aeruginosa produce EPS consisting of mannuronic, glucuronic, and nucleic acids, and small amounts of proteins (Eagon, 1956; 1962; Brown et al., 1969; Evans

and Linker, 1973; Mian et al., 1978).

Bacterial EPS have been shown to be involved in selective accumulation of ions (Galanos et al., 1977; Leive, 1974). Turakhia et al. (1983) stimulated biofilm detachment by chelation of calcium ions, and Turakhia (1986) reported decreasing cellular detachment with increasing calcium availability. Turakhia (1986) concluded that calcium ions contribute to biofilm cohesiveness through the cross-linking of EPS.

EPS has been categorized based on its spatial association with the bacterial cell; a) capsule, which is a compact layer attached to the cell, and b) slime, which is a dispersed layer loosely associated with the cell (Brock, 1979). Due to the somewhat arbitrary distinction between slime and capsule, a quantitative separation would be difficult, and has not been attempted in previous biofilm studies (Trulear, 1983; Turakhia, 1986). Bakke (1983) stimulated EPS detachment without influencing cell detachment, suggesting the presence of at least two categories of EPS with different functions. One kind of EPS ties the cells together in the biofilm, while an other portion of the EPS has a different, unknown, function which is influenced by substrate loading rate transitions. Christensen et al. (1986) isolated and characterized two soluble EPS produced by a marine pseudomonas, and found that the relative production rates of the two EPS changed from

the exponential growth phase to the stationary state in batch cultures. Sutherland (1977) and Costerton et al. (1978) claim that EPS play at least two significant roles in 1) structure of microbial aggregate and 2) transfer processes between cells and the environment, supporting the presence of at least two functionally different EPS. Electron micrographs were applied in this study to seek an EPS categorization based on its functional role in biofilms.

Organism

The strain of Pseudomonas aeruginosa used in this study was obtained from the culture collection of the Department of Microbiology at Montana State University (Bozeman, MT). This organism has been studied extensively in both dispersed and biofilm cultures (Trulear, 1983; Robinson et al., 1984; Bakke et al., 1984; Turakhia et al., 1986). Kinetic and stoichiometric coefficients for this organism is presented in Table 1. Other characteristics describing P. aeruginosa include: a) negative gram stain (Buchanan et al., 1974), b) strict aerobe (Buchanan et al., 1974), c) chemoorganotroph (Buchanan et al., 1974), d) rod shape (Buchanan et al., 1974), e) can cause severe infections in a compromised host (Woods et al., 1980; Costerton, 1979), f) its primary mode of growth is in colonies attached to surfaces (e.g. infections) (Costerton, 1979).

Biofilm-Liquid Interface

Erosion and sloughing are distinguished partly by their different effects on biofilm morphology. Erosion separates small particles from the biofilm surface by fluid shear force. The "peaks" of a rough biofilm surface are, therefore, more exposed to erosion, and erosion tends to smooth the biofilm-liquid interface. A smoother interface leads to decreased mass and fluid shear stress. If, as

Table 1. Relevant kinetic and stoichiometric coefficients for P. aeruginosa.

Coef.	Value	Units	Source
m_m	0.4	h^{-1}	Robinson <u>et al.</u> (1984)
K_{gS}	2.0	$g_S m^{-3}$	"
k_{gP}	0.27	$g_P g_M^{-1}$	"
k_{nP}	0.035	$g_P g_M^{-1} h^{-1}$	"
Y_{PS}	0.56	$g_P g_S^{-1}$	"
Y_{MS}	0.34	$g_M g_S^{-1}$	"

Howell and Atkinson (1976) suggested, substrate limitations in the film cause sloughing, then decreased substrate flux into the film due to smoothing by erosion may lead to sloughing. Removal of biofilm in large pieces during sloughing will lead to increased biofilm roughness, which,

in turn, increases mass transport and fluid shear stress. Increased fluid shear stress may, in turn, lead to increased erosion. Therefore, erosion may enhance sloughing and vice versa, so that most biofilms will reach some balance between the two processes. A biofilm will display a rougher biofilm-liquid interface when sloughing, as opposed to erosion, is the dominating process. A rough interface does not, however, imply that sloughing is the dominating detachment process because several other factors, such as biofilm composition, can also influence biofilm interface morphology.

Increased frictional resistance to fluid flow due to biofilm roughness has been observed (Trulear and Characklis, 1982). This implies greater fluid shear stress and, according to Equation 1, higher detachment rate. Filamentous organisms impose, in general, much greater friction on the liquid flow than do non-filamentous biofilm cultures (Trulear and Characklis, 1982). So, biofilm interface morphology is important for both momentum and mass transfer between the liquid and the biofilm phase and was a main focus of this study.

THEORY

ModelMass balance

A system can be divided into m phases. Accumulation of compounds within each phase is described by a balance equation of the general form:

$$\begin{array}{l} \text{net rate of} \\ \text{accumulation} \\ \text{within the} \\ \text{phase} \end{array} = \begin{array}{l} \text{net rate of} \\ \text{transport} \\ \text{into the} \\ \text{phase} \end{array} + \begin{array}{l} \text{net rate of} \\ \text{transformation} \\ \text{within the} \\ \text{phase} \end{array} \quad 2$$

Equation 2 can be expressed in vector form (Roels, 1980; Bakke et al. 1984; Wanner and Gujer, 1985). In the k th phase:

$$(d(C_{ij})/dt)_k = N_{ijk} + R_{ijk} \quad 3$$

where: C = chemical state vector

N = flux vector for net transport into phase k

R = intraphase production rate vector

i = component 1,2,3... h

j = process 1,2,3... l

k = phase 1,2,3... m

The time progression of the components is determined by simultaneous integration of Equation 3 over all i , j , and k , which can be done by numerical analysis.

Multiplying Equation 3 by the elemental composition matrix of the system yields an elemental balance, which may be very useful in stoichiometric analysis (Roels, 1980). This matrix contains the number of atoms of the atomic species considered per mole of component i .

Phase separation

A system can be divided into a number of distinct phases depending on physical characteristics, requirements of model resolution, and available computing capacity. The most simple case, $m = 1$, is appropriate for ideal continuous flow stirred tank reactors (CFSTR), or chemostats, in which all activity resides in a homogeneous liquid phase. Plug flow reactors can be modeled as CFSTRs in series and then $m > 1$, since each CFSTR is considered a separate phase. If a biofilm exists in a CFSTR, then it is appropriate for $m \geq 2$, since a liquid phase and one or more biofilm phases exist. Layers in a biofilm with distinct biological activity may be modeled as different phases within a system. A biofilm can, for example, be regarded as several interacting layers perpendicular to the main diffusion gradient, where each layer of thickness L_{fk} is described by mass balances for

phase k . By increasing the number of layers m for a given biofilm thickness L_f , the thickness of each layer, L_{fk} , decreases. If $m \rightarrow \infty$ then $L_{fk} \rightarrow 0$ and the mass balances for the biofilm becomes a partial differential equation in z and t , which can be applied to predict cellular distribution, activity, and diffusion gradients within biofilms (Wanner and Gujer, 1984).

The mass balance model (Equation 3), applied to a two phase system ($m = 2$), consisting of one biofilm phase (phase 2, $k = 2$) and one bulk liquid phase (phase 1, $k = 1$) is schematically described in Figure 1. The coordinate system defined for this analysis, where x is the bulk flow direction, and z is perpendicular to the substratum, is also described in this figure. Both theoretical and experimental analysis of this system has been performed (Bakke et al., 1984; 1986) yielding mass balances for substrate, cell, and EPS (Table 2). These equations are used extensively in this study, because the experimental system used here is identical to that analyzed by Bakke et al. The same system has also been analyzed in terms of the more complex situation $m \rightarrow \infty$ (Wanner and Gujer, 1985; Wanner, personal communication), yielding information on gradients in the film.

Sensitivity Analysis

Monoculture biofilms were simulated by simultaneous integration of the mass balances in Table 2 by a numerical 4-th order Runge-Kutta routine on a VAX 11/750 computer to determine which parameters are more significant to biofilm progression (Bakke et al., 1986). Kinetic and stoichiometric coefficients for biofilm processes published by Robinson et al. (1984), Nelson et al. (1985), and Bakke et al. (1984) were applied in this biofilm simulation. It was demonstrated in this sensitivity analysis that, even though cellular adsorption to the substratum is a prerequisite for biofilm formation, biofilm progression beyond the very early stages of biofilm formation is quite insensitive to the magnitude of the process (Bakke et al., 1986). Adsorption processes were, therefore, not accounted for in this study, reducing the number of terms in the mass balances. The resulting mass balances, including kinetic and stoichiometric coefficients for the processes, are presented in Table 3. Coefficient values for transformation processes by P. aeruginosa, determined in chemostats, applied in the computer simulations are listed in Table 1.

Figure 1. Schematic representation of two phase biofilm system described by Equations 10-15. Bulk transport, substrate diffusion, cell and EPS production, and detachment are processes included. The coordinate system defined for this study is illustrated.

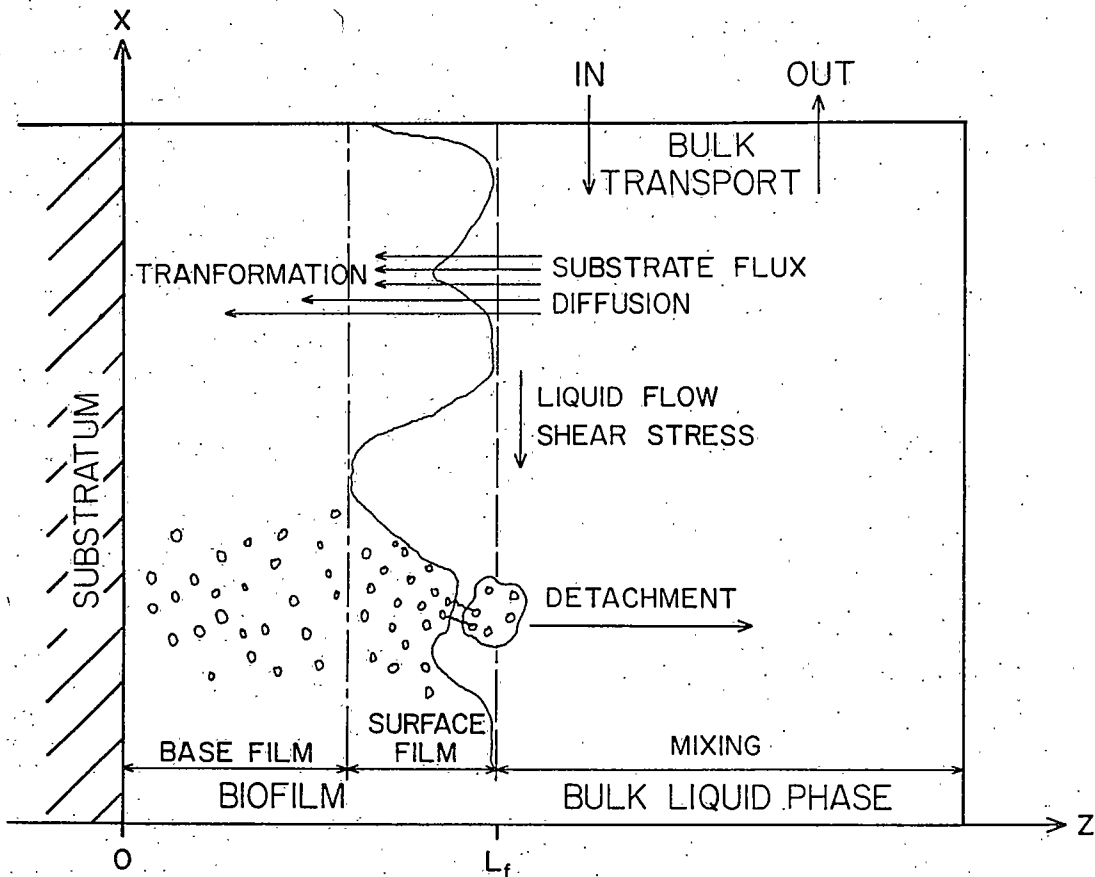


Table 2. Mass balances for biofilm reactor with general terms for process rates.

Liquid Phase Substrate (Eq. 4);

$$\frac{dC_{S1}}{dt} = (C_{S0} - C_{S1})D - C_{M2}r_S - C_{M1} \left[\frac{m}{Y_{MS}} + \frac{r_P}{Y_{PS}} \right]$$

Liquid Phase Cell (5);

$$\frac{dC_{M1}}{dt} = (C_{M0} - C_{M1})D + C_{M2}r_{dM} + C_{M1}m - C_{M1}r_{aM}$$

Liquid Phase Products (6);

$$\frac{dC_{P1}}{dt} = (C_{P0} - C_{P1})D + C_{P2}r_{dP} + C_{M1}r_P$$

Biofilm Substrate (7);

$$\frac{dC_{S2}}{dt} = C_{M2}r_S - C_{M2}f_D \left(\frac{m}{Y_{MS}} + \frac{r_P}{Y_{PS}} \right)$$

Biofilm Cell (8);

$$\frac{dC_{M2}}{dt} = -C_{M2}r_{dM} + C_{M2}f_D m + C_{M1}r_{aM}$$

Biofilm Products (9);

$$\frac{dC_{P2}}{dt} = -C_{P2}r_{dP} + C_{M2}f_D r_P$$

Table 3. Mass balances for biofilm reactor including kinetic expressions for specific rates (Bakke et al., 1984).

Liquid Phase Substrate (10);

$$\frac{dC_{S1}}{dt} = DC_{S1}D - C_{M2}r_S - C_{M1} \left[\frac{m_m C_{S1}}{K_{gS} + C_{S1}} \left(\frac{1}{Y_{MS}} + \frac{k_{gP}}{Y_{PS}} \right) + \frac{k_{nP}}{Y_{PS}} \right]$$

Liquid Phase Cell (11);

$$\frac{dC_{M1}}{dt} = -C_{M1}D + C_{M2}r_{dM} + C_{M1} \frac{m_m C_{S1}}{K_{gS} + C_{S1}}$$

Liquid Phase Product (12);

$$\frac{dC_{P1}}{dt} = -C_{P1}D + C_{P2}r_{dP} + C_{M1} \left[k_{gP} \left(\frac{m_m C_{S1}}{K_{gS} + C_{S1}} \right) + k_{nP} \right]$$

Biofilm Substrate (13);

$$\frac{dC_{S2}}{dt} = 0 = C_{M2}r_S - C_{M2}f_D \left[\frac{m_m C_{S1}}{K_{gS} + C_{S1}} \left(\frac{1}{Y_{MS}} + \frac{k_{gP}}{Y_{PS}} \right) + \frac{k_{nP}}{Y_{PS}} \right]$$

Biofilm Cell (14);

$$\frac{dC_{M2}}{dt} = -C_{M2}r_{dM} + C_{M2}f_D \frac{m_m C_{S1}}{K_{gS} + C_{S1}}$$

Biofilm Product (15);

$$\frac{dC_{P2}}{dt} = -C_{P2}r_{dP} + C_{M2}f_D \left(k_{gP} \frac{m_m C_{S1}}{K_{gS} + C_{S1}} + k_{nP} \right)$$

Process Rates

This section explains the manipulations and assumptions applied to the mass balances in Table 3 in order to derive measurable expressions for the individual processes. Kinetics are expressed in terms of specific process rates (units = t^{-1}). Separating the effects of growth and detachment on biofilm accumulation is of particular interest.

A balance of specific rates is obtained by dividing the biofilm cell mass balance (Equation 14) by biofilm cell mass, C_{M2} :

$$\frac{1}{C_{M2}} \frac{dC_{M2}}{dt} = -r_{dM} + m_2 \quad 16$$

where the left hand side (l.h.s.) of Equation 16 is the specific cellular accumulation rate in the biofilm. r_{dM} is the specific cellular detachment rate. m_2 is the average specific cellular growth rate in the biofilm. The specific cellular accumulation rate can be obtained by measuring cell mass with time.

Specific cellular detachment rate, r_{dM} , can be determined from the liquid phase cell balance (Equation 11) given liquid phase substrate mass and cell mass in both

phases. The need for liquid phase substrate mass data can be eliminated by supplying high reactor surface area to volume ratio and liquid dilution rate, D , so that growth rate in the liquid phase can be neglected (Bakke et al., 1984). Solving Equation 11 for specific cellular detachment yields:

$$r_{dM} = (D C_{M1} - dc_{M1}/dt) / C_{M2} \quad 17$$

At steady state, Equation 17 simplifies to:

$$r_{dM} = D C_{M1} / C_{M2} \quad 18$$

Average specific biofilm cellular growth rate, m_2 , can be estimated from liquid phase specific cellular growth rate, m_1 :

$$m_2 = f_D m_1 \quad 19$$

where f_D is an effectiveness factor for substrate diffusion ($0 < f_D < 1$), which depends on the diffusivity of the substrate, substrate concentration, and biofilm density (Atkinson and Davies, 1974). Values for m_1 can be calculated after Monod (1940),

$$m_1 = m_m C_{S1} / (K_{gS} + C_{S1}) \quad 20$$

given maximum cellular growth rate, m_m , cellular growth saturation coefficient, K_{GS} , and liquid phase substrate concentration, C_{S1} . m_m and K_{GS} for P. aeruginosa are listed in Table 1.

An expression for m_2 can also be obtained from the biofilm substrate balance, which, due to the short characteristic time for substrate diffusion in biofilms, can be assumed at steady state (Hermanowicz and Ganczarczyk, 1985):

$$m_2 = \frac{r_S - k_{nP}/Y_{PS}}{1/Y_{MS} - k_{gP}/Y_{PS}} \quad 21$$

where r_S is specific substrate flux into the biofilm. k_{gP} and k_{nP} are growth and non-growth associated polymer formation rate coefficients, respectively. Y_{PS} and Y_{MS} are stoichiometric yields for products (EPS) and cells from substrate, respectively (Table 1). r_S can be obtained from the liquid phase substrate balance (Equation 10), which, assuming negligible activity in the liquid phase and steady state, yields:

$$r_S = D \Delta C_{S1} Y_{MS} / C_{M2} \quad 22$$

where $\Delta C_{S1} = C_{S0} - C_{S1}$

Biofilm Composition

To avoid contamination and physical disturbance of the system, the biofilm in this study was sampled only at the end of the experiments. Indirect measures of biofilm composition were, therefore, sought.

Rearranging Equation 18 yields:

$$C_{M2} = C_{M1} D / r_{dM} \quad 23$$

Applying the same assumptions (steady state and insignificant activity by the suspended cells) to the liquid phase product balance:

$$C_{P2} = C_{P1} D / r_{dP} \quad 24$$

According to Wanner and Gujer (1984), r_{dM} equals r_{dP} in a homogeneous biofilm at steady state. Experimental data also show $r_{dM} = r_{dP}$ (Bakke et al., 1984). Combining Equations 23 and 24, therefore, yields

$$\frac{C_{M2}}{C_{P2}} = \frac{C_{M1}}{C_{P1}} \quad 25$$

The ratio of cells to polymers in the biofilm can, in other words, be estimated from their ratio in the liquid phase at steady state. Equation 25 can also serve as a good estimate for non-steady state conditions as long as the accumulation terms are negligible compared to detachment rates.

An important condition for coexistence of particulate species (e.g. cells and EPS) in biofilms at steady state (O. Wanner, personal communication) is that the specific production rates must be the same for all coexisting species at the substratum. Therefore:

$$m = r_p \quad \text{at} \quad z = 0 \quad 26$$

where m as a function of substrate concentration is described by Equation 20 and specific product formation rate can be described by (Bakke et al., 1984):

$$r_p = (k_{gP} m + k_{nP}) C_{M2} / C_{P2} \quad 27$$

m and $(r_p C_{P2} / C_{M2})$ are plotted vs. substrate concentration in Figure 2 based on the coefficients in Table 1. So, given Equation 26, the following inequalities emerge:

$$\text{when } m > r_P C_{P2} / C_{M2} : C_{M2} > C_{P2} \quad 28$$

and

$$\text{when } m < r_P C_{P2} / C_{M2} : C_{M2} < C_{P2} \quad 29$$

where, from Figure 2, Inequality 28 is valid for $C_S > 0.25$ and 29 for $0 < C_S < 0.25$ at the substratum. These inequalities relate biofilm composition to metabolic conditions (i.e. cell to EPS mass ratio vs. substrate concentration). Note that the transition value for C_S ($= 0.25 \text{ g m}^{-3}$) depends strongly on k_{nP} , and the magnitude of k_{nP} is rather uncertain (Trulear, 1983; Robinson et al., 1984; Turakhia, 1986). Note also that if $C_S = 0$ at the substratum then inequalities 28 and 29 are not valid, and from Equations 26 and 27:

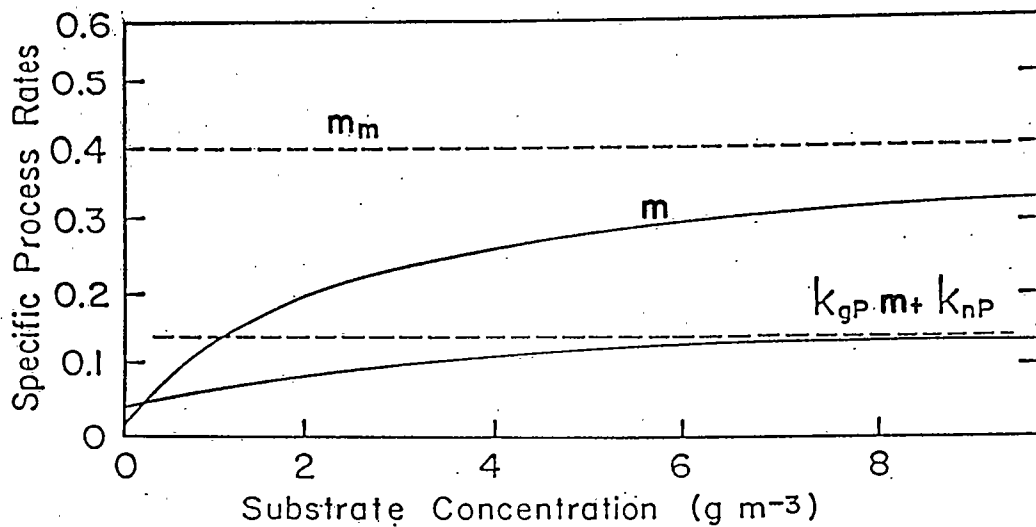
$$k_{nP} C_{M2} / C_{P2} = 0 \quad 30$$

at the substratum. Equation 30 is satisfied if there are no cells at the substratum, or if $k_{nP} = 0$, as suggested by Turakhia's (1986) data.

Simulation of experiments published by Bakke et al. (1984) did not correlate well with data in terms of EPS content in the biofilm (Wanner, personal communication). This suggested that the EPS production coefficients

determined by Robinson et al. (1984) (Table 1) were inaccurate. Increasing the non-growth associated product formation coefficient, k_{np} , significantly improved the fit of simulation to data (Wanner, personal communication). Turakhia, however, found that k_{np} was not significantly different from zero, an apparent contradiction to Wanner's results. This apparent contradiction is analyzed the Discussion chapter in light of data obtained in this study.

Figure 2. Specific cellular growth rate, m , modeled as a saturation function of substrate concentration and product formation rate modeled as the sum of a growth and a non-growth associated term, plotted vs. substrate concentration.



EXPERIMENTAL METHODS

Methods were developed to obtain biofilm thickness and density data non-intrusively and non-destructively. A biofilm reactor was constructed to accommodate the methods which are described in detail in this chapter. Methods previously published are referenced.

Experimental Apparatus

The experiments were conducted in a mixed rectangular tube reactor (MRTR) described in Figures 3, 4, and 5, and Tables 4 and 5. Figure 3 is a schematic diagram of the entire experimental apparatus describing liquid and air flow and temperature control. The reactor (Figure 4) is a recycle loop with air and liquid inflow ports and a combined effluent. The air travels the shortest distance from the inflow to the outflow ports and not through the rectangular tube loop to avoid an additional (gas) phase in the system. The air flow supplies oxygen to the water, mixes the liquid phase, and rapidly transports liquid between the influent port and the effluent port. A peristaltic pump drives the recycle flow through the rectangular (pyrex) tubes. One of these tubes is equipped with a manometer to measure pressure

drop due to friction at the biofilm-liquid interface. Samples were obtained at locations labeled 1 through 8.

The rectangular tubes were constructed from a square and a rectangular capillary tube as described by the cross section view (Figure 5). The capillary tube was sealed and fastened to the center of the square tube by silicone glue at both ends, creating two parallel rectangular channels as the liquid phase. The rectangular channels are 1.9x5.0x300 mm. The coordinate system is defined in Figure 5, and sampling locations for biofilm thickness profiles are labeled along the y-axis. Thickness measurements (in the z direction) were obtained at $y = -1.00, -0.75, \dots, 1.00$ mm.

Characteristic dimensions and parts description for the MRTR are listed in Tables 4 and 5.

Operating Conditions

Both bulk liquid transport conditions (i.e. mixing and flow rates) and liquid phase composition (i.e. influent nutrient, temperature, buffer etc.) were carefully controlled to maintain constant environmental conditions. The only parameter varied during an experiment was recycle flow rate, which was varied as a step function in time, imposing the fluid shear force progressions described in Figures 6, 7, and 8 for the three specific experiments.

Figure 3. Schematic diagram of experimental system including flow and temperature control for gas and liquids.

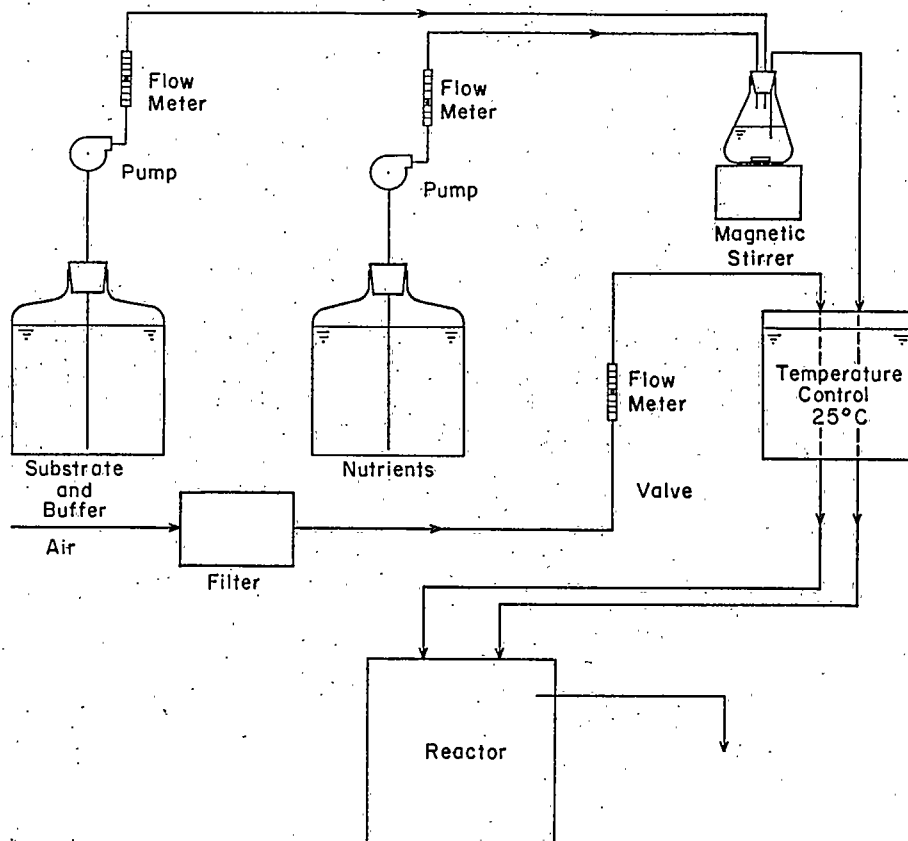


Figure 4. Mixed rectangular tube reactor (MRTR). Biofilm measurements and samples were obtained at locations labeled 1-8.

